SAILING THROUGH SPECTRA: UNVEILING THE POTENTIAL OF MULTI-SPECTRAL INFORMATION IN MARINE DEBRIS SEGMENTATION

Dyutit Mohanty * † **Aditya Kasliwal** * **Bharath Udupa** * **Pratinav Seth** *

ABSTRACT

Plastic debris in ocean waters poses ecological and economic challenges. Addressing this issue begins with estimating plastic distribution in oceans for effective policy and awareness efforts. Traditional monitoring methods are costly and labour-intensive, with limited coverage. Deep learning models using multispectral remote sensing data show promise in overcoming these limitations. However, accurately distinguishing floating plastic from other sea surface features remains challenging. In our work, we use the multi-spectral Sentinel-2 MARIDA dataset to explore the impact of various spectral feature combinations on the performance of deep learning models for segmenting marine plastic in the presence of other sea surface features. This innovative approach improves accuracy and serves as an open benchmark for multi-spectral marine debris segmentation.

1 INTRODUCTION AND PREVIOUS WORKS

The world's oceans receive more than 19 million tonnes of plastic waste annually (UNEP), posing threats to aquatic wildlife, marine ecosystems, and human health. Despite growing awareness, urgent attention is required as the amount of plastic litter entering the oceans continues to rise (Vered & Shenkar, 2021). A key factor in addressing marine plastic pollution is accurate monitoring of its distribution in the ocean. Accurate monitoring allows decision-makers to create effective policies to target highly polluted areas (Copernicus) and heightens public awareness of the issue's urgency, encouraging the adoption of responsible waste management and citizen advocacy for policy changes (Soares et al., 2021). Conventional methods like on-site sample collection for monitoring waterborne plastics are costly, labour-intensive, and offer limited coverage (Hafeez et al., 2018). This data scarcity impedes our understanding of plastic quantities and longevity in aquatic ecosystems. Deep learning models using remote sensing data overcome these constraints, bridging the gap in marine pollution knowledge. Numerous studies have employed machine/deep learning models for ocean plastic monitoring. Sannigrahi et al. (2022) utilized SVM and Random Forest models with input as FDI, PI, and NDVI spectral indices. Mifdal et al. (2021) employed various machine learning algorithms and a U-Net architecture using FDI and NDVI. Additionally Basu et al. (2021) employed a range of models, including supervised (SVR), unsupervised (K-means, FCM), and semi-supervised (SFCM), with NDVI and FDI as input. A commonality in these works is the use of spectral indices in the input to aid models in distinguishing floating plastic from other sea surface features. In our study, we focus on the input features and explore the impact of different spectral feature combinations on a U-Net's performance in detecting ocean plastic amid various sea surface features. We experiment with diverse combinations of 8 spectral indices, 11 spectral signatures, and 6 Gray Level Co-Occurrence Matrices. Notably, our study stands out as the first to focus on the impact of multi-spectral information, demonstrating its potential by significantly enhancing model accuracy.

2 METHODOLOGY AND RESULTS

We use the MARIDA (Marine Debris Archive) dataset (Kikaki et al., 2022), which contains multi-spectral Sentinel-2 satellite images of coastal waters. The dataset contains classes for the various sea

*Manipal Institute of Technology, Manipal Academy of Higher Education, Manipal, India
†Corresponding Author - dyutitmohanty407@gmail.com

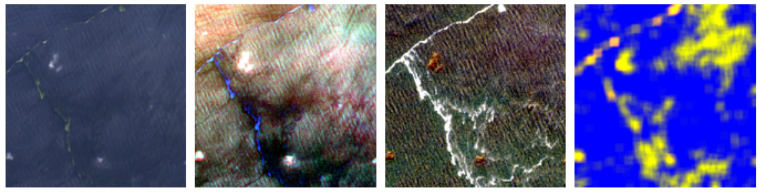

Figure 1: Base ocean image captured by Sentinel-2, Ocean image with 11 spectral signatures, Ocean image with 8 spectral indices, Ocean image with 6 GLCM features

surface features that coexist with marine plastic (such as algae, ships, and waves). Certain classes in the dataset contain considerably more annotated pixels than others, and to mitigate this class imbalance, we conducted experiments involving reduced class subsets. Our experiments encompassed two class sets: Subset 1: MD - Marine Debris (floating plastics/polymers), DenS & SpS - dense and sparse Sargassum algae, NatM - floating organic materials, SWater – shallow water; Subset 2 integrates Ships, Foam, and Waves, in addition to the classes from Subset 1. Subset 1 highlights marine debris in optimal coastal conditions with minimal class imbalance. Subset 2 extends the evaluation, introducing more classes for a comprehensive assessment but with increased imbalance. For each image, 11 spectral signatures were extracted. A spectral signature represents the radiation reflected off a surface as a function of wavelength (ESA). This information aids in identifying different surface types. Additionally, 8 spectral indices were calculated. A spectral index is a mathematical expression that combines data from different wavelengths in an image to enhance specific information about the Earth's surface (Sykas). It does this by analyzing spectral reflectance in various bands. Lastly, a Grey Level Co-occurrence Matrix (GLCM) with 6 features was extracted. The GLCM objectively describes the texture of a surface (rough or smooth) and is the joint probability distribution of the grey levels of pixel pairs (Zheng et al., 2018). 'Our experimental framework utilises the U-Net (Ronneberger et al., 2015), a standard encoder-decoder network. The input layer was modified to accommodate additional channels, incorporating various combinations of spectral signatures, indices, and GLCM textures, all stacked and presented as input to the network. Our experimentation involved three different input channel configurations: 11 channels (solely spectral signatures), 19 channels (comprising spectral signatures and spectral indices), and 25 channels (encompassing spectral signatures, spectral indices, and GLCM textures). Due to the uneven class distribution, we experimented with several loss functions, opting for Dice Loss alongside Cross-Entropy Loss.

Table 1: IoU and F1-scores for Marine Debris across different input modalities for Subset 1.

Input Modalities	Loss	IoU	F1 - Score
SIGNATURES	DICE	0.74	0.85
	CE	0.68	0.81
+ INDICES	DICE	0.54	0.70
	CE	**0.86**	**0.92**
+ TEXTURES	DICE	0.84	0.91
	CE	0.79	0.88

Table 2: IoU and F1-scores for Marine Debris across different input modalities for Subset 2.

Input Modalities	Loss	IoU	F1 - Score
SIGNATURES	DICE	0.64	0.78
	CE	0.48	0.65
+ INDICES	DICE	0.73	0.85
	CE	**0.80**	**0.89**
+ TEXTURES	DICE	0.77	0.87
	CE	0.57	0.73

Due to dataset imbalance, we assessed model performance using the F1 score in addition to IoU. In Table 1, combining spectral signatures and indices using Cross-Entropy Loss achieves the highest Subset 1 F1-Score. Table 2 shows a decline in Subset 2 performance with additional classes, but the spectral signature-indices pair exhibits the least decline. Across other input configurations, Dice Loss generally enhances performance, except for the spectral signature-indices setup. Similarly, for IoU performance, using spectral signatures and indices paired with Cross-Entropy produces the best results. The decline in performance when integrating all channels may be due to noisy GLCM textures. This study demonstrates the potential of multi-spectral information in enhancing deep learning model performance in distinguishing ocean plastic from sea surface features. Our benchmark results confirm the effectiveness of this approach, aiding accurate plastic detection for monitoring and policy decisions. Despite promising results, the model's generalisation may be challenged by the uneven geographical distribution of data, particularly in regions with phenomena resembling floating plastic, such as jellyfish blooms. To address this, future exploration could involve training with diverse marine datasets akin to MARIDA's objectives. Employing self-supervised learning can leverage abundant unlabeled satellite data, contributing to a more even geographic image distribution. Experimentation with smaller input channel subsets may further enhance model performance.

3 URM STATEMENT

The authors acknowledge that at least one key author of this work meets the URM criteria of the ICLR 2023 Tiny Papers Track. All the authors' ages lie outside the range of 30-50 years; geographically, they are not located in North America, Western Europe, the UK, or East Asia, and they are of non-White race. Three authors are first-time submitters to a conference of the stature of ICLR.

REFERENCES

Bidroha Basu, Srikanta Sannigrahi, Arunima Sarkar Basu, and Francesco Pilla. Development of novel classification algorithms for detection of floating plastic debris in coastal waterbodies using multispectral sentinel-2 remote sensing imagery. *Remote Sensing*, 13(8):1598, 2021.

Copernicus. Detecting plastic pollution. URL https://marine.copernicus.eu/explainers/phenomena-threats/plastic-pollution/detecting-plastic-pollution.

ESA. Spectral signatures. https://www.esa.int/SPECIALS/Eduspace_EN/SEMPNQ3Z2OF_0.html.

Sidrah Hafeez, Man Sing Wong, Sawaid Abbas, Coco YT Kwok, Janet Nichol, Kwon Ho Lee, Danling Tang, and Lilian Pun. Detection and monitoring of marine pollution using remote sensing technologies. *Monitoring of Marine Pollution*, 2018.

Katerina Kikaki, Ioannis Kakogeorgiou, Paraskevi Mikeli, Dionysios E Raitsos, and Konstantinos Karantzalos. Marida: A benchmark for marine debris detection from sentinel-2 remote sensing data. *PloS one*, 17(1):e0262247, 2022.

Jamila Mifdal, Nicolas Longépé, and Marc Rußwurm. Towards detecting floating objects on a global scale with learned spatial features using sentinel 2. *ISPRS Annals of the Photogrammetry, Remote Sensing and Spatial Information Sciences*, pp. 285–293, 2021.

Olaf Ronneberger, Philipp Fischer, and Thomas Brox. U-net: Convolutional networks for biomedical image segmentation. In *Medical Image Computing and Computer-Assisted Intervention–MICCAI 2015: 18th International Conference, Munich, Germany, October 5-9, 2015, Proceedings, Part III 18*, pp. 234–241. Springer, 2015.

Srikanta Sannigrahi, Bidroha Basu, Arunima Sarkar Basu, and Francesco Pilla. Development of automated marine floating plastic detection system using sentinel-2 imagery and machine learning models. *Marine Pollution Bulletin*, 178:113527, 2022.

Joana Soares, Isabel Miguel, Cátia Venâncio, Isabel Lopes, and Miguel Oliveira. Public views on plastic pollution: Knowledge, perceived impacts, and pro-environmental behaviours. *Journal of hazardous materials*, 412:125227, 2021.

Dimitri Sykas. Spectral indices in remote sensing and how to interpret them. https://www.geo.university/pages/spectral-indices-in-remote-sensing-and-how-to-interpret-them.

UNEP. Plastic pollution. URL https://www.unep.org/plastic-pollution.

Gal Vered and Noa Shenkar. Monitoring plastic pollution in the oceans. *Current Opinion in Toxicology*, 27:60–68, 2021.

Gang Zheng, Xiaofeng Li, Lizhang Zhou, Jingsong Yang, Lin Ren, Peng Chen, Huaguo Zhang, and Xiulin Lou. Development of a gray-level co-occurrence matrix-based texture orientation estimation method and its application in sea surface wind direction retrieval from sar imagery. *IEEE Transactions on Geoscience and Remote Sensing*, 56(9):5244–5260, 2018.

A Appendix

A.1 Dataset

The dataset consists of image patches of coastal waters gathered over several years (2015-2021) from various locations around the globe. Initially, reports on marine litter and plastic pollution from several different countries were gathered to serve as ground-truth data. These reports included observations from citizen scientists, social media, and ocean clean-up efforts. Based on the ground-truth data, Sentinel-2 remote sensing images were acquired. The images were then manually annotated by image interpretation experts.

The dataset contains 15 classes: MD (marine debris consisting of floating plastics or other polymers, mixed anthropogenic debris), DenS (dense floating Sargassum macroalgae), SpS (sparse floating Sargassum macroalgae), NatM (natural materials such as vegetation & wood), Ship (sailing & anchored vessels), Cloud (clouds including thin clouds), MWater (clear marine water), SLWater (sediment-laden water which is high sediment river discharges with brown color), Foam (foam recorded at riverfronts or coastal wave breaking area), TWater (turbid waters close to coastal areas), SWater (coastal waters, including coral reefs and submerged vegetation), Waves, CloudS (cloud shadows), Wakes (wakes & waves from a sailing vessel) and MixWater (water near floating materials).

MARIDA consists of 1381 patches, with 837,357 annotated pixels. The image patches and their corresponding masks are provided in GeoTIFF format. For each scene 11 spectral signatures were extracted: nm440, nm490, nm560, nm665, nm705, nm740, nm783, nm842, nm865, nm1600, nm2200. In addition to this, 8 spectral indices were also calculated: NDVI, NDWI, FAI, FDI, SI, NDMI, BSI, and NRD. A Gray Level Co-occurrence Matrix was also extracted with 6 features: Contrast (CON), Dissimilarity (DIS), Homogeneity (HOMO), Energy (ENER), Correlation (COR), and Angular Second Moment. These are referred to as ”textures”.

A.2 Training Details and Results Across all Classes

We used U-Net to perform our experiments. VGG16 with ImageNet pretrained weights was used as the encoder. Each model underwent training for a total of 44 epochs, employing a batch size of 5. The initial learning rate was set at 2x10-4 and was subsequently reduced to 2x10-5 following the 40th epoch. We used the ADAM optimizer to minimize the loss in our experiments. Additionally, random rotations (-90°, 0°, 90°, or 180°) were applied to the input images as part of the training process. Additional results across all individual class configurations for both subsets are in Table 3 and Table 4. The code is available at: `https://github.com/dyutitmohanty/MARIDA_PLASTIC_DECTECTION`.

Table 3: IoU scores across different classes and input modalities for Subset 1.

Input Modalities	Loss	MD	DenS	SpS	NatM	Swater	mIoU
SIGNATURES	Dice	0.74	0.75	0.75	0.09	0.94	0.65
	CE	0.68	0.81	0.80	**0.38**	0.94	0.72
+ INDICES	Dice	0.54	0.60	0.52	0.15	**0.99**	0.56
	CE	**0.86**	0.80	0.83	0.28	**0.99**	**0.75**
+ TEXTURES	Dice	0.84	0.80	0.78	0.20	0.97	0.72
	CE	0.79	**0.84**	**0.85**	0.32	0.97	**0.75**

Table 4: IoU scores across different classes and input modalities for Subset 2.

Input Modalities	Loss	MD	DenS	SpS	NatM	Swater	Ship	Foam	Waves	mIoU
SIGNATURES	Dice	0.64	0.83	0.79	0.18	0.92	**0.92**	0.42	0.73	0.68
	CE	0.48	0.82	0.75	0.4	0.83	0.91	0.69	0.76	0.71
+ INDICES	Dice	0.73	0.84	**0.84**	0.17	**0.95**	0.72	0.48	0.77	0.69
	CE	**0.80**	**0.86**	0.83	**0.27**	0.94	0.74	0.40	0.79	0.70
+ TEXTURES	Dice	0.77	0.83	**0.84**	0.14	0.94	0.88	0.62	**0.84**	0.73
	CE	0.57	0.82	0.83	0.00	0.93	0.81	**0.74**	0.82	**0.79**